# Engineering Tool for Temperature, Electric Field and Dose Rate Dependence of Low Conductivity Spacecraft Materials

JR Dennison[1], Alec Sim[2], Jerilyn Brunson[2], Jodie Gillespie[2], Steven Hart[3], Justin Dekany[3], Charles Sim[3], and Dan Arnfield[3]
*Physics Department, Utah State University, Logan, UT, 84325*

**An engineering tool has been developed to predict the equilibrium conductivity of common spacecraft insulating materials as a function of electric field, temperature, and adsorbed dose rate based on parameterized, analytic functions derived from physics-based theories. The USU Resistivity Calculator Engineering Tool calculates the total conductivity as the sum of three independent conductivity mechanisms: a thermally activated hopping conductivity, a variable range hopping conductivity, and a radiation induced conductivity using a total of nine independent fitting parameters determined from fits to an extensive data set taken by the Utah State University Materials Physics Group. It also provides a fit for the temperature dependence of the electrostatic breakdown field strength, in terms of a tenth independent fitting parameter related to an interchain bond strength. The extent of F, T and $\dot{D}$ measured in the experiments were designed to cover as much of the ranges typically encountered in space environments as possible. This Mathcad worksheet calculates the total conductivity and the individual contributions from each conductivity mechanism based on user inputs for F, T and $\dot{D}$. It also plots 2D and 3D graphs of the conductivities over the appropriate full ranges of F, T and $\dot{D}$.**

## Nomenclature

| | | |
|---|---|---|
| $a$ | = | average nearest neighbor trap separation |
| $\dot{D}$ | = | absorbed radiation dose rate |
| $E_b$ | = | energy difference between top of conduction band and the steady-state Fermi level due to irradiation |
| $E_C$ | = | energy of the bottom of the conduction band |
| $E_F$ | = | energy of the dark current Fermi level |
| $E_F'$ | = | energy of the steady-state Fermi level due to irradiation |
| $E_{gap}$ | = | band gap energy, energy difference between top of conduction band and the top of the valence band |
| $E_o$ | = | energy difference between top of conduction band and the dark current Fermi level |
| $E_V$ | = | energy of the top of the valence band |
| $F$ | = | electric field |
| $F_A$ | = | thermally activated hopping reduced E-field scaling factor |
| $F_{ESD}$ | = | electrostatic breakdown field strength |
| $F_V$ | = | variable range hopping reduced E-field scaling factor |
| $f$ | = | number of conduction electrons excited by the high energy radiation per unit volume and time |
| $k_{RIC}$ | = | temperature-dependant RIC proportionality constant |
| $k_{RICo}$ | = | temperature-independent RIC magnitude |
| $k_{RIC1}$ | = | the temperature-dependent RIC magnitude |
| $m_e^*$, $m_h^*$ | = | electron and hole effective masses |
| $n$ | = | density of free carriers |
| $n_b$ | = | distribution of trapped states exponentially decreasing below the conduction band edge |
| $N_{E_F}$ | = | mean energy density of trapped states at energy $E_F$ |

[1] Professor, Physics Department, UMC 4415, Senior Member.
[2] Graduate Student, Physics Department, UMC 4415.
[3] Undergraduate Student, Physics Department, UMC 4415.

$N$ = energy density of trapped states
$P$ = transition probability to break an interchain bond in electrostatic breakdown
$q_c$ = charge per carrier
$q_e$ = charge per electron
$R$ = variable range separation of trapped states
$s$ = capture cross section of conduction electrons by fixed holes
$t_{en}$ = endurance time or mean time to failure in electrostatic breakdown
$T$ = temperature
$T_A$ = thermally activated hopping reduced temperature scaling factor
$T_V$ = variable range hopping reduced temperature scaling factor
$T_{RIC}$ = the reduced RIC temperature scaling factor, the temperature at which traps were "frozen in" as the material cooled
$\alpha$ = real space decay constant of the localized state wave function
$\beta_A$ = the ratio of field energy to thermal energy for thermally activated hopping conductivity
$\beta_V$ = the ratio of field energy to thermal energy for variable range hopping conductivity
$\Delta$ = temperature-dependant power for standard RIC power-law equation
$\Delta G$ = change in Gibbs free energy for a rupture of interchain van der Waals bonds or the activation energy of the chain deformation or micro-void formation process in electrostatic breakdown
$\Delta H$ = energy separation of trapped states for hopping conductivity
$\Sigma$ = mean energy required to create conduction electron through collision of high energy radiation
$\lambda$ = the maximum size of submicrocavities involved in electrostatic breakdown
$\mu$ = carrier mobility
$\nu_{TAC}$ = hopping frequency for thermally activated hopping conductivity
$\nu_{VRH}$ = hopping attack frequency for variable range hopping conductivity
$\rho_m$ = mass density
$\sigma$ = the conductivity (the ratio of current density to electric field)
$\sigma_{RIC}$ = radiation induced conductivity (RIC)
$\sigma_{TAH}$ = thermally activated hopping (TAH) conductivity
$\sigma_{TAHo}$ = thermally activated hopping reduced conductivity scaling factor
$\sigma_{VRH}$ = variable range hopping (VRH) conductivity
$\sigma_{VRHo}$ = variable range hopping reduced conductivity scaling factor

## I. Introduction

THE ubiquity of highly insulating materials in the design of spacecraft and many other technology components places special emphasis on understanding and modeling the electrical properties of these insulators, which are critical for anticipating and preventing potentially damaging charging phenomena.[1-3] The complex relationships between spacecraft insulators and their surroundings are fundamentally based on a detailed knowledge of how individual materials store and transport charge. The low charge mobility of insulators causes charge to accumulate where deposited, preventing uniform redistribution of charge and creating differential local electric fields and potentials. Effects of local potential differences can range from any number of systematic errors, arcing to external plasmas, and—in the extreme case—complete system failure due to a charge pulse generated by breakdown of the insulating materials.[1,3,4] Further, long-term accumulation of charge can cause degradation of exterior surfaces, enhance contamination of the materials, and cause inaccuracies in measurement or information storage. The history of the sample becomes important as the behavior of the material is modified with further charging.[5-7]

The conductivity of a material is a key transport parameter in determining how deposited charge will redistribute throughout the system, how rapidly charge imbalances will dissipate, and what equilibrium potential will be established under given environmental conditions.[8] Developing a better understanding of the physics of insulating materials, increasing the versatility and reliability of charge transport models, and expanding the database of information for the electronic properties of insulating materials can assist designers in accommodating and mitigating these harmful effects.[2] Specifically, as the requirements for space missions extend to new regions of space and more stringent requirements are placed on spacecraft performance, it becomes necessary to better understand the underlying conduction mechanisms that determine the response of insulators to temperature, electric field and dose rate.

## II. Engineering Tool

The objective of this study has been to develop an engineering tool to predict the equilibrium conductivity, $\sigma$, of common spacecraft insulating materials as a function of electric field $F$, temperature $T$, and adsorbed dose rate $\dot{D}$ over ranges typically encountered in the space environment. Parameterized, analytic functions from physics-based theories used to model the dependence of the conductivity on $F$, $T$ and $\dot{D}$ are described in detail in Section III. Conductivity data sets are measured at limited combinations of $F$, $T$ and $\dot{D}$ designed to span the space environment ranges as much as possible and are fit to the theoretical functions. In analytic form, these functions can then be used to interpolated to other combinations of the independent variables $F$, $T$ and $\dot{D}$ within the measured range and—with extreme caution—to extrapolate outside the ranges explored by direct measurements.

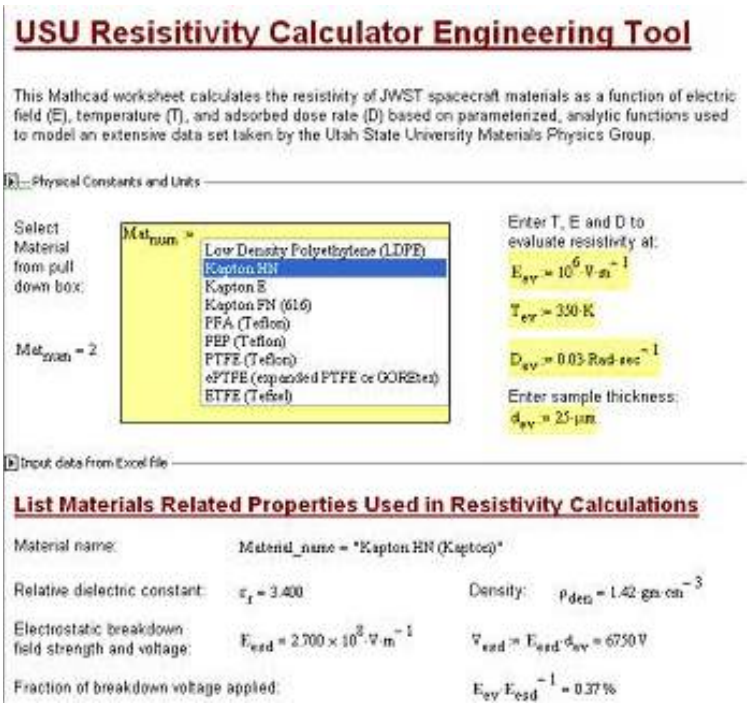


**Figure 1. Mathcad engineering tool user input interface.** *Required user inputs, highlighted in yellow, are limited to material type, electric field, temperature, absorbed dose rate and sample thickness. Conductivity fitting parameters and other materials properties such as dielectric constant and mass density are retrieved from an accompanying database file.*

Figure 1 shows the input interface for the second generation USU Resistivity Calculation Engineering Tool. The tool is a Mathcad worksheet that calculates the total conductivity based on only minimal user inputs. Models of the conduction mechanisms have physics-based materials parameters. The engineering tool also plots 2D and 3D graphs of the conductivities over the appropriate ranges of independent variables $F$, $T$ and $\dot{D}$ (see examples in Section IV), allowing intuitive visual analysis.

The engineering tool calculates the total conductivity as the sum of three independent conductivity mechanisms: thermally activated hopping (TAH) conductivity, variable range hopping (VRH) conductivity and radiation induced conductivity (RIC). The models of these mechanisms are based on hopping conductivity models developed and validated for disordered semiconductor materials, and are applied here to spacecraft insulator materials as semi-empirical models. To perform fits to measured data, it is more convenient to make a conversion from the standard physics-based model parameters to reduced notation where conductivity, temperature and electric field are expressed in reduced units. In addition, the temperature dependence of the electrostatic breakdown field strength, $E_{ESD}$, at a specified endurance time (related to the ramp rate at which $E_{ESD}$ is measured), is expressed in terms of the TAH conductivity model and its fitting parameters. There are a total of ten independent fitting parameters:

- three ($\sigma_{TAHo}$, $T_A$, and $F_A$) to scale the thermally activated hopping reduced conductivity, reduced temperature and reduced E-field, respectively;
- three ($\sigma_{VRHo}$, $T_V$, and $F_V$) to scale the variable range hopping reduced conductivity, reduced temperature and reduced E-field, respectively;
- three ($k_{RICo}$, $k_{RIC1}$ and $T_{RIC}$) to scale the temperature-independent RIC magnitude, the temperature-dependent RIC magnitude, the reduced RIC temperature.; and
- one ($F_{A'}$) to scale the thermally activated interchain bond strength.

The range of validity of the conductivity values predicted by the engineering tool are largely determined by the ranges of the experimental data sets used to determine the fitting parameters. Values of the fitting parameters used by the engineering tool are largely based on an extensive data set taken by the Utah State University Materials Physics Group.[5,7,9]

Dark current conductivity data are typically measured over temperature ranges from ~120 K to 345 K at a low E-field and a high E-field. For some of the materials in the USU database, the dark current conductivity at room temperature has also been measured with the charge storage method.[4-6,9,10]

Reasonable dark current conductivity data is typically available at room temperature over the broad range of electric fields from $<10^5$ V-m$^{-1}$ (where conductivity is essentially independent of electric field) up to ~$10^7$ V-m$^{-1}$ or from <0.05% up to between 30% to 90% of the electrostatic breakdown field strength, $F_{ESD}$ (see Section III. D for details). Electrostatic breakdown field strength is also measured independently, typically at room temperature and at a voltage ramp rate of 20 V/s at 1 sec intervals. In many cases $F_{ESD}$ is also measured as a function of temperature[11] from ~150 K to ~300 K and at different voltage ramp rates[12] up to the limit of 500 V/s suggested in ASTM 3755.[13] The E-field conductivity and $E_{ESD}$ measurements taken together provide a reasonable coverage of the full E-field range.

RIC has typically been measured at absorbed dose rates from $10^{-5}$ Gray to $10^{-1}$ Gray at several fixed temperatures from 150 K to 330 K.[11,14] The range of absorbed dose rate in the USU tests was roughly on the order of that spanned by average to storm solar wind fluxes in the near-Earth environment, although other space conditions or shielding can lead to dose rate exposures one to two orders of magnitude above or below the measured range. Fortunately, there is substantial evidence that RIC in the measured ranges can be accurately extrapolated from near zero dose rate to $>10^1$ Gray for the materials studied.[15]

For most highly insulating materials tested, the range of valid conductivity data is determined by the lower limits of currents measurable by the constant voltage test apparatus [ref], on the order of $10^{-15}$ A to $10^{-14}$ A; this typically corresponds to an lower bound in measurable conductivities of $10^{-18}$ Ω-cm to $10^{-20}$ Ω-cm and charge decay times of days to about a year.[5,7] Where available, charge storage measurements have been used to extend these limits down to equilibrium conductivities of $10^{-19}$ Ω-cm to $10^{-21}$ Ω-cm and charge decay times of weeks to about a decade.[4,5] Therefore, for some materials valid conductivity measurements could not be made at lower temperatures or dose rates. For most materials studied, variable range hopping was not observed in the range of conductivities that were experimentally accessible. Further, one has to recognize that extrapolation to temperatures outside the range of valid conductivity measurements can lead to erroneous results if structural phase transitions, such as the glass transition temperature, occur. Caution must also be exercised since conductivity and $F_{ESD}$ are also known to depend to varying degrees on sample preparation and contamination, sample thickness, radiation damage, stored space charge, and sample conditioning.[16]

Finally, it must be recognized that the theories used for the engineering tool are for equilibrium conductivities, in the limit where all transient response has come to an end. Transient conductivity can include polarization effects and space charge effects of diffusive charge.[7,17] In insulators a displacement conduction mechanism results from the time dependant response of dielectric materials to an applied electric field. No net charge is transferred across the material; rather the transient dielectric current results primarily from the reorientation of molecular dipoles and the movement of ionic charge from one part of the sample to another in response to the applied field. For insulators diffusion often describes the spread of injected carriers into trapped states within the material. Space charge effects can be significant as traps are filled with injected charge and inhibit further motion of the carriers. Diffusion of particles to lattice sites often leads to a power law model of the time dependence of this conduction. For the materials tested, polarization transients typically take seconds to tens of minutes to reach equilibrium, in most cases well within the experimental times allowed for the samples to come to equilibrium. However, for the materials tested the times required for space charge to come to diffusive equilibrium can be hours to days, often in excess of the experimental times allowed for the samples to come to equilibrium. Fortunately, in most cases the difference between the dark current conductivities measured at longest times and the true equilibrium conductivities are small, typically less than a factor of 2. USU RIC experiments waited sufficient time to reach equilibrium; RIC typically came to equilibrium from 5 to 20 minutes after the dose rate was adjusted to a higher value. While USU $F_{ESD}$ experiments used voltage ramp rates ~ 25 times less than required by ATSM guidelines,[13] equilibration times were often inadequate to correctly model endurance times appropriate for samples in the space environment that can approach mission lifetimes in some circumstances. Breakdown fields for very long exposure times were estimated to be from 2 to 10 times lower than those measured be the USU experiments.[18]

## III. Theoretical Model

Conductivity, $\sigma$, is a measure of the transport of charged particles under the influence of an applied electric field within a material. For conduction by charge transport through a material, the conductivity (the ratio of current density to electric field, $\sigma=J/F$) is given as the product of the charge per carrier $q_c$, density of carriers $n$, and carrier

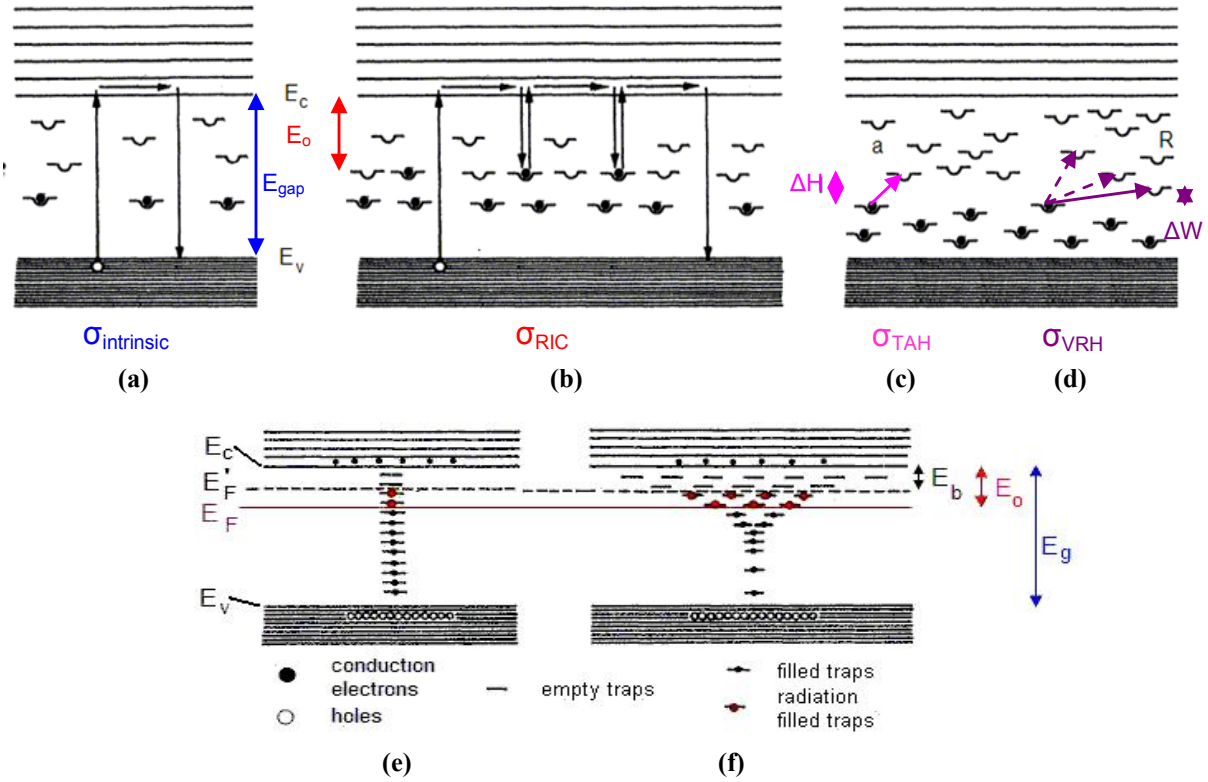


**Figure 2. Model of conduction in insulating materials. (a)** *Extended state conductivity in intrinsic semiconductors.* **(b)** *Thermal assisted trap state conduction.* **(c)** *Thermally assisted hopping conduction.* **(d)** *Variable range hopping conduction.* **(e)** *uniform and* **(f)** *exponential energy distribution of localized trap states. Energies along the vertical axes noted are: $E_C$, bottom of conduction band; $E_F'$, steady-state Fermi level due to irradiation; $E_F$, dark current Fermi level; $E_V$, top of valence band; $E_b \equiv E_C - E_F'$; $E_o \equiv E_C - E_F$; $E_{gap} \equiv E_C - E_V$; and $\Delta H$ or $\Delta W$, energy separations of trapped states. Distances along the horizontal axes noted are: a, average nearest neighbor trap separation; R, variable range trap separation.*

mobility $\mu$, as $\sigma = q_c n \mu$. In steady-state conditions, both $n$ and $\mu$ can depend on the magnitudes of $F$ or $T$ and reflect the electronic structure of the material.

The primary conduction mechanism for conductors involves intraband excitation of electrons from filled extended states to empty extended states at only slightly higher energy within the same conduction band; this mechanism is not available to insulators since there are no empty states within the valence band (*i.e.*, $n \rightarrow 0$).

Charge transport in intrinsic semiconductors is primarily via thermally activated interband excitation of electrons from extended states in the valence band to extended states in the conduction band with an activation energy equal to the band gap energy, $E_{gap}$ (see Figure 2(a)). However, this conduction mechanism is negligible in insulators at reasonable working temperatures (again, $n \rightarrow 0$); indeed, the distinction between semiconductors and insulators is that thermally activated transitions between extended states are highly improbable in insulators, because the band gap energy separating the states is much larger than the average thermal energy of the electrons. In well-ordered semiconductors these states are extended states, but can be localized for topologically (structurally) disordered states or chemically disordered (*e.g.*, dopant or intrinsic defect) states. While this reduces the activation energy to as little as the separation between the conduction and valence band mobility edges, the gap is still much larger than the thermal energy.

The charge transport properties of insulators are significantly different from those of conductors and semi-conductors, and in general involve fundamentally different conduction mechanisms. Theoretical models of conductivity in highly insulating materials, such as the polymers or ceramics, are most often based on hopping conductivity models involving localized trapped states. The key information to characterize a given material in such models is the number, occupation and distribution in energy, $n(F;T)$, of the localized states found within the band gap between the top of the valence band and the bottom of the conduction band. These models were most often developed for disordered semiconducting materials, and have been shown to be quite effective in describing electron transport in these types of semiconductors.[19] However, for highly insulating materials—and polymers in

particular—the applicability and the validity of the assumptions inherent in these models are unclear. For example, trapping sites in highly disordered polymeric materials are not uniform and evenly spaced and have higher densities than in semiconductors. The limited experimental evidence to date suggests that the hopping conductivity models do, in fact, describe some basic features of polymers.[17]

Below we consider the equilibrium conductivity as the sum of three conduction mechanisms involving localized states that are active in insulators: the steady-state conductivity due to thermally activated hopping (TAH) $\sigma_{TAH}$ (see Figure 2(c)), variable range hopping (VRH) $\sigma_{VRH}$ (see Figure 2(d)), and photoexcitation or radiation induced conductivity (RIC) $\sigma_{RIC}$ (see Figure 2(b)):

$$\sigma_{Total}(F,T,\dot{D}) = \sigma_{TAH}(F,T) + \sigma_{VRH}(F,T) + \sigma_{RIC}(\dot{D},T) \tag{1}$$

When $\sigma_{RIC}$ is not active, the remaining conductivity is referred to as the dark current conductivity. As discussed below, the behavior is simplified in that $\sigma_{TAH}$ and $\sigma_{VRH}$ are by definition independent of $\dot{D}$ and $\sigma_{RIC}$ is found to be independent of $F$.

The theories used here for explaining electrical behavior in insulating polymers are based on multiple trap hopping conductivity models developed to understand charge transport in disordered semiconductors and amorphous solids.[17,20-24] These theories assume that electrons or holes are the primary charge carriers and that their motion through the material is governed by availability of a distribution of localized states treated as potential wells or energy traps on a lattice. They are well tested for semiconductors, but remain largely unverified for insulators, in large part because it is difficult to appropriately define the nature of localized states used to determine carrier density and mobility in materials with such complex molecular structure and extreme disorder.[17,22,23] Concentrations of impurity atoms or chains are difficult to quantify; the polymer chains do not lend themselves to the simplifications of a lattice construct and have myriad structural internal degrees of freedom; and polar groups attached to the chains, cross linking and broken bonds have significant influence on carrier mobility.[17,21] These polar groups can also contribute to an overall material polarization that influences the internal electric field felt by the carriers.[25,26]

Numerous extensions of these basic theories to more complex descriptions of insulator conduction involving more accurate representations of the localized states, charge carrier dynamics, and more complete models of charge carrier transport exist; some are briefly noted below. Arkhipov[20,21] and Tyutnev[22,23] and Bassler[24] were instrumental in the development of the Gaussian Dynamics Model (GDM) based on charge dynamics equations; they wer able to show direct connections to the multiple trapping models.[27-30] Mott and Davis,[27] Anderson,[30] Scher and Montroll,[32] and Dunlap[33] made key advances in statistical mechanics transport models based on hopping and random walks on disordered lattices that have been subsequently extended to percolation theory; these advances are also central to understanding dark current and radiation-induced charge transport in disordered semiconductors and insulators modeled below. Excellent reviews are available of the work in this field over the last more than fifty years.[21-24] However, in a broad sense, these more advanced theories do not substantially alter the dependences of conductivities on $F$, $T$ and $\dot{D}$ that underlie the basic behaviors modeled in this engineering tool. Therefore, for the sake of clarity and simplicity, we restrict our development to basic multiple trapping and hopping models.

### A. Thermally Activated Hopping Conductivity

The theory of thermally activated hoping conductivity[A14] $\sigma_{TAH}$, originally formulated for charge transport in ionic crystals,[34] provides a model for the temperature and electric field dependence of hopping conductivity. For example, it can model the thermal excitation of charge carriers trapped in shallow wells (localized states) below the conduction band into extended states in the conduction band, which are subsequently retrapped in shallow localized states (see Figure 2(b)). Here the carrier mobility is proportional to a Boltzmann factor with the energy scale set by trap depth, $\Delta H$, times a Boltzmann factor with energy scale $\pm q_e Fa$ gained (lost) by a charge carrier moving with (against) the electric field over a distance of the average trap separation $a$ (see Figure 2(c)).[35] Mott[27] theory for TAH conductivity assumes that: (i) all charge carriers are electrons (e.g., holes are assumed immobile), (ii) electrons in the extended states of the conduction band act as nearly free electrons, and (iii) space charge is negligible (e.g., only bulk effects are considered and the bulk is charge neutral).

The standard form of $\sigma_{TAH}(F,T)$ (ref. 14) for thermally activated hopping conductivity has three physics-based parameters, the product $N(T)\cdot\nu_{TAH}$ that sets the conductivity magnitude, the activation energy $\Delta H$ that sets the low temperature behavior or energy scale, and the mean separation between hopping states, $a$, that sets the intermediate E-field behavior or the length scale.[17] Alternately, this standard form can be expressed in terms of a conductivity scaling factor $\sigma_{TAHo}$, a temperature scaling factor $T_A$, and an electric field scaling factor $F_A$ as:

$$\sigma_{TAH}(F,T) = \left[\frac{2N(T)\nu_{TAH}\, a\, q_e}{F}\right] \exp\left[\frac{-\Delta H}{k_B T}\right] \sinh\left[\frac{a\, q_e\, F}{k_B T}\right] = \left\{\sigma_{TAHo}(T)\left(T_A/T\right) Z_A(\beta_A) \exp\left(-T_A/T\right)\right\} \tag{2}$$

where the ratio of field energy to thermal energy is

$$\beta_A \equiv 4F\, T_A / 3\, F_A\, T = q_e\, F\, a / k_B T \qquad with \quad Z_A(\beta_A) \equiv 1/\beta_A \sinh(\beta_A) \tag{3a}$$

and

$$\sigma_{TAHo}(T) \equiv 2\, N(T)\, \nu_{TAH}\, q_e^{\,2}\, a^2, \qquad T_A \equiv \Delta H / k_B \qquad and \qquad F_A \equiv 4\Delta H / 3 q_e\, a \tag{3b}$$

$\sigma_{TAHo}(T)$ is proportional to the frequency of hops, $\nu_{TAH}$, and can have a weak temperature dependence through energy density of trapped states, $N(T)$.

Figure 3 illustrates the general behavior of $\sigma_{TAH}(F,T)$ as a function of reduced temperature and reduced electric field. At low electric fields $<10^6$ V/m, Eq. (2) is independent of $F$ and exhibits a $T^{-1}exp(T^{-1})$ dependence; that is at low electric fields, $Z_A \rightarrow 1$. In the range of ~$10^6$ V/m to $10^7$ V/m Eq. (2) is approximately linear in $F$. At still higher fields of $>10^8$ V/m, Eq. (2) becomes temperature independent and exhibits an $F^{-1}exp(F)$ $E$-field dependence. At largest electric fields near $F_{ESD}$, the TAH conductivity model diverges to much higher conductivities. The relation between Eq. (2) and $F_{ESD}$ is discussed further in Section III. D.

Numerous alternative models for the high electric field dependence have been developed.[17] For example, application of a large electric field across the sample distorts the potential well and lowers the activation energy needed for the electron to hop the potential barrier;[17,27] this enhanced conductivity leads to the so-called Poole-Frenkel factor[26] where $\beta_{PF}$ is the Poole-Frenkel coefficient that depends only on the charge of the carrier and the dielectric constant of the material, assuming a coulombic potential well.[7,36] Note that at low electric fields, $\sigma_{PF} \rightarrow \sigma_{TAHo}$. The Poole-Frenkel model is only a rough approximation, which has been extended in many way;[17] of particular importance is application of the Onsanger solution treating steady-state diffusion of carriers between trapped states.[17]

### B. Variable Range Hopping Conductivity

The VRH conductivity mechanism developed by Mott and Davis[25,27] models charge transport from one localized state to another, through thermally activated quantum mechanical tunneling (see Figure 2(d)). It is often applied to a distribution of deeper trap states, such as localized impurity states within the band gap, where promotion to extended states is highly unlikely. Here the carrier mobility is proportional to the product of a Boltzmann factor with the energy scale set by the difference in trap depth of the localized states involved in the tunneling, $\Delta W$, and a tunneling probability, $exp(2R\alpha)$; this second term is proportional to the square of an exponent of the ratio of the well separation (or barrier width), $R$, to the

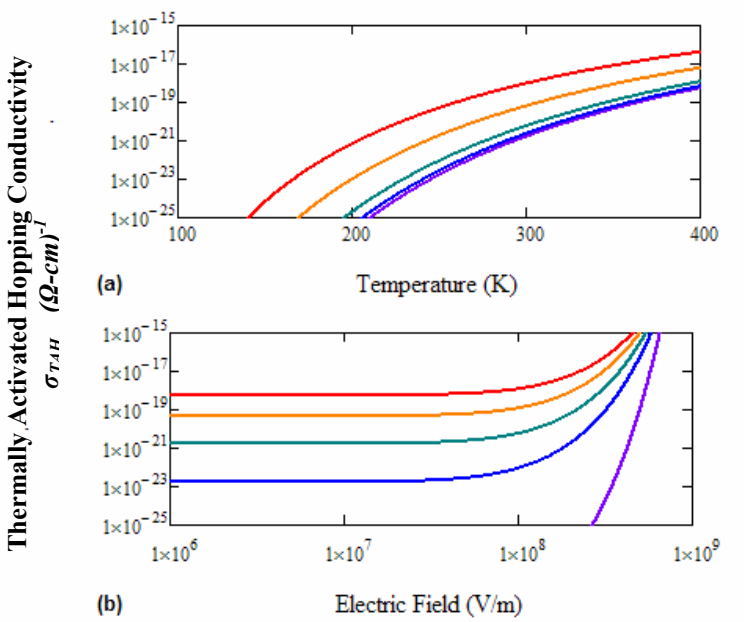


**Figure 3. Temperature and electric field dependence of thermally activated hopping conductivity. (a)** *Temperature dependence with electric fields of $1{\cdot}10^7$ V/m (purple), $5{\cdot}10^7$ V/m (blue), $1{\cdot}10^8$ V/m (green), $2{\cdot}10^8$ V/m (orange) and $3{\cdot}10^8$ V/m (red).* ***(b)*** *Electric field dependence with temperatures of 150 K (purple), 250 K (blue), 300 K (green), 350 K (orange) and 400 K (red). Curves are based on Eq. (2). To approximately match LDPE data we have set $\sigma_{TAHo}=1.4{\cdot}10^{-10}$ $(\Omega\text{-cm})^{-1}$ and $F_A=9.5{\cdot}10^8$ V/m for $T_A=6626$ K. $F_{ESD}$ is ~$3{\cdot}10^8$ V/m.*

localization length of the states (or wave function decay length), $\alpha^{-1}$. The possibility that an electron can tunnel to a more distant neighboring well with a larger energy difference leads to a more gradual decrease in conductivity, resulting in a $T^{-1/4}$ dependence in the exponent for 3-dimensional solids. This means that, even though the density of localized defect states in the gap that contribute to $\sigma_{VRH}$ is usually much less than for the localized states in the conduction band mobility edge that contribute to $\sigma_{TAH}$, there is the possibility that $\sigma_{VRH}$ can be dominant at low T.

The standard physics-based model for variable range hopping from the original work by Mott and Davis[27]—as extended by Apsley and Hughes[36,37] to include electric field dependence—can be expressed in terms of a constant energy density of states, $N_{E_F}$; a hopping attack frequency, $\nu_{VRH;}$ and a real space decay constant of the localized state wave function, α. The Apsley and Hughes model can alternately be expressed in terms of a conductivity scaling factor $\sigma_{VRHo}$, a temperature scaling factor $T_V$, and an electric field scaling factor $F_V$ as:

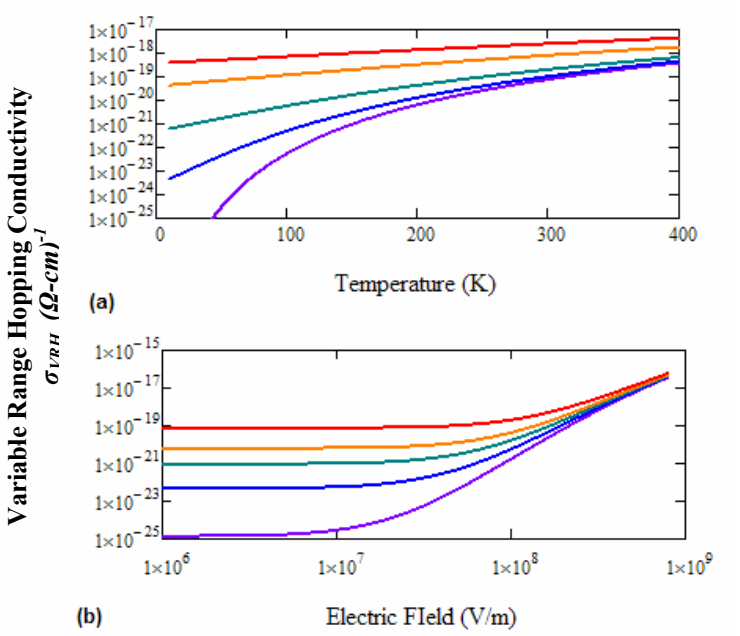


**Figure 4. Temperature and electric field dependence of variable range hopping conductivity. (a)** *Temperature dependence with electric fields of $1{\cdot}10^7$ V/m (purple), $5{\cdot}10^7$ V/m (blue), $1{\cdot}10^8$ V/m (green), $2{\cdot}10^8$ V/m (orange) and $3{\cdot}10^8$ V/m (red).* ***(b)*** *Electric field dependence with temperatures of 50 K (purple), 100 K (blue), 150 K (green), 200 K (orange) and 300 K (red). Curves are based on Eq. (4). To approximately match LDPE data we have set $\sigma_{VRHo}=1.0{\cdot}10^{-10}$ $(\Omega\text{-cm})^{-1}$ and $F_V=6.9{\cdot}10^{13}$ V/m for $T_V=1.0{\cdot}10^8$ K.*

$$\sigma_{VRH}(F,T)=\left\{\sigma_{VRHo}(T)\left(T_V/T\right)^{1/4} Z_{V1}(\beta_V)\exp\left[\left(-T_V/T\right)^{1/4} Z_{V2}(\beta_V)\right]\right\} \tag{4}$$

$$\text{with}\quad \sigma_{VRHo}(T)=2\,N_{E_F}\,\nu_{VRH}\,q_e^{\,2}/(2\alpha)^2,\quad T_V\equiv 3(2\alpha)^3/N_{E_F}\pi k_B\quad \text{and}\quad F_V\equiv 4(2\alpha)^4/N_{E_F}\pi q_e$$

where the ratio of field energy to thermal energy is in analogy with Eq. (3),

$$\beta_V\equiv 4FT_V/3F_V T=q_e F(2\alpha)^{-1}/k_B T \tag{5}$$

$\sigma_{VRH}$, $T_V$ and $F_V$ have the same functional form as the TAH parameters in Eq. (3b), but with a mean energy density of trap states $N_{E_F}=[(3/\pi)\,(\Delta H/(2\alpha)^{-3})]$ at energy $E_F$ and mean trap separation of $(2\alpha)^{-1}$. Note that both $Z_{V1}$ and $Z_{V2}$ are complex polynomial functions of $\beta_V$ and that at low electric fields, both $Z_{V1}\rightarrow 1$ and $Z_{V2}\rightarrow 1$.[38] These functions are defined as

$$Z_{V1}(\beta_V)\equiv\left[2/Z_{Vo}(\beta_V)\right]^{1/4}\quad\text{and}\quad Z_{V2}(\beta_V)\equiv\left(\frac{-1}{2\beta_V}\right)\cdot\left[1+\frac{Z_{Vo}(\beta_V)}{Z_{Vo}(\beta_V)-\frac{3}{2}\beta_V}\right]\cdot Z_{V1}(\beta)\cdot\left[\frac{\frac{3+\beta_V}{24\cdot(1+\beta_V)^3}-\frac{1}{8}-\frac{\beta_V}{3}}{\frac{2+\beta_V}{6\cdot(1+\beta_V)^2}+\frac{1}{3}+\frac{\beta_V}{2}}\right] \tag{6}$$

$$\text{with}\quad Z_{Vo}(\beta_V)\equiv\frac{\left(1+\beta_V/2\right)}{(1+\beta_V)^2}+\left(1+\frac{3}{2}\beta_V\right)$$

Figure 4 illustrates the general behavior of $\sigma_{VRH}$ as a function of reduced temperature and reduced electric field. At low electric fields $<10^6$ V/m, Eq. (4) is independent of $F$ and exhibits a $T^{-1/4}exp(T^{-1/4})$ dependence; that is at low

electric fields, $Z_{V1} \rightarrow 1$ and $Z_{V2} \rightarrow 1$. In the range of ~$10^6$ V/m to $10^7$ V/m Eq. (4) is approximately linear in $F$. At still higher fields of >$10^8$ V/m, Eq. (4) becomes temperature independent and exhibits a $F^{-1/4}exp(F^{-1/4})$ dependence.

### C. Radiation Induced Conductivity

A third steady-state conduction mechanism—called photoconductivity or radiation induced conductivity (RIC)—involves excitation of carriers into extended states from either extended or localized states by external influences (see Figure 2(b)). This includes electron photoexcitation by light or by high energy radiation including electrons, ions and photons. RIC is the enhancement in conductivity of a material due to deposition of energy by incident high energy radiation. As insulators are bombarded with a flux of high energy radiation, the large energy of the incident particles is shared with many bound (valence) electrons within the material that are excited into higher energy levels in the conduction band, in a manner analogous to the effects of thermal energy on dark current conductivity. The conductivity of the material is therefore enhanced by the absorbed energy per unit mass (dose, $D$), rather than by direct charge deposition from the incident radiation. This is illustrated by various studies of RIC versus radiation dose rate, $\dot{D} \equiv \partial D / \partial t$.[15]

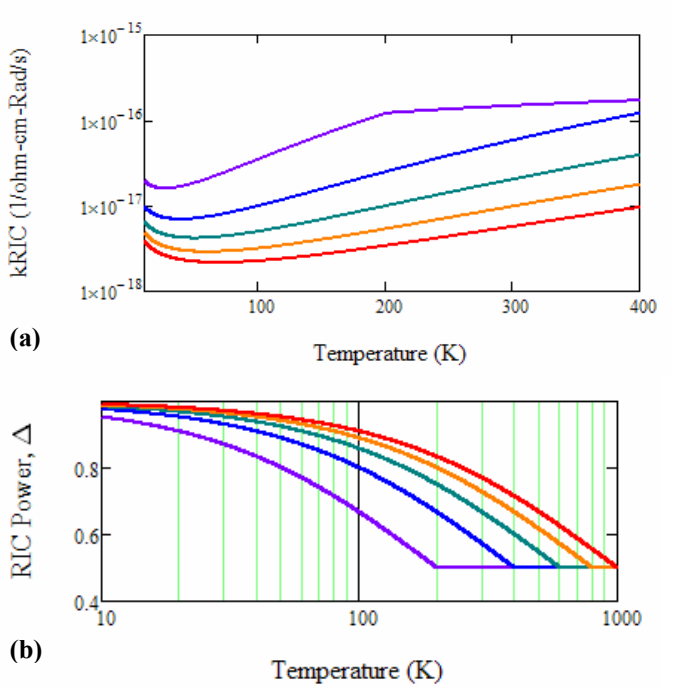


**Figure 5. Temperature dependence of the RIC parameters. (a)** *Proportionality constant, $k_{RIC}$, based on Eq. (8). (b) RIC power, $\Delta$, based on Eq. (7). Values shown are for $T_{RIC}$ set to 200 K (purple), 400 K (blue), 600 K (green), 800 K (orange) and 1000 K (red). To approximately match LDPE data we have set $k_{RICo}=1.8 \cdot 10^{-14}$ $(\Omega\text{-cm-Rad/sec})^{-1}$ and $k_{RIC1}=4.6 \cdot 10^{-5}$ for $T_{RIC}=600$ K.*

Standard theories of RIC predict that $\sigma_{RIC}$ is proportional to $\dot{D}$ raised to the power $\Delta$,

$$\sigma_{RIC}(\dot{D}) = k_{RIC}(T)\, \dot{D}^{\Delta(T)} \tag{7}$$

with proportionality constant, $k_{RIC}$.[17,28,39] Both $k_{RIC}$ and $\Delta$ are material dependent parameters, that can in general depend on $T$. $k_{RIC}$ for most organic dielectrics are typically up to two or more orders of magnitude smaller than inorganic dielectrics.[17] $\Delta$ usually lies between 0.5 and 1.0, with higher values being more common.[17] As with hopping conductivity models, we expect that $\sigma_{RIC}$ will be proportional to the number of charge carriers.[17,28] At higher fluxes and incident energies, the radiation can produce new traps via radiation damage, leading to enhanced conductivity;[40] such dependence typically occurs at $10^4$ Gray or more for polymers[15] and so will not be considered here.

A theory of steady state photoconductivity in disordered semiconductors was developed by Rose that predicts the $\dot{D}$ dependence of $\sigma_{RIC}$ and the $T$ dependence of the proportionality constant, $k_{RIC}(T)$ and power $\Delta(T)$.[40] Rose extended the basic TAH theory (see Figure 2(a)) to model excitation of electrons from the valence band into the conduction band by high energy radiation and their subsequent decay into a distribution of localized trapped states with energies near the bottom of the conduction band (see Figure 2(b)). Fowler adapted this to model RIC and made connections to rate equations for charge carriers and excitations.[28,29] As with Mott theory for thermally activated hopping conductivity, the Rose,[41] Fowler[28,29] and Vaiserburg[42] (RFV) theory assume that only electron conduction is considered (e.g., holes are assumed immobile), that electrons in the extended states of the conduction band act as nearly free electrons, and that space charge is negligible (e.g., only bulk effects are considered and the bulk is charge neutral). RIC is predicted to depend on the energy distribution of the trapped states within the conduction band and the occupancy of these states, as well as the mean lifetimes of the photocarriers in the conduction band and the electrons in the trapped states. By arguing that in equilibrium: (i) the rate of carriers excited by the radiation from the valence band into the conduction band must equal the rate of recombination of these photoelectrons with stationary holes (ii) that high energy radiation acts to completely fill additional trapped states up to the steady-state

Fermi level due to irradiation, $E_F'$, (iii) the number of conduction electrons excited by the high energy radiation per unit volume and time $f = \dot{D}\rho_m / \Sigma$, and (iv) the distribution of trapped states is uniformly spaced in energy below the conduction band edge (see Figure 2(e)), Rose showed that $\Delta \rightarrow 1$ and $k_{RIC}$ is independent of $T$, so that $\sigma_{RIC}$ is independent of $T$ and linearly proportional to $\dot{D}$. However, when the distribution of trapped states exponentially decreased below the conduction band edge (see Figure 2(f)) as $n_b(E)=n_o exp(-E_b/k_B T_{RIC})$ at a rate scaled by $T_{RIC}$, which is equal to the temperature at which traps were "frozen in" as the material cooled, Rose found that:

$$\Delta(T) = \left[1 + T/T_{RIC}\right]^{-1} \tag{8}$$

and

$$k_{RIC}(T) = q_e \mu_o \left[\left(\frac{\rho_m}{s\Sigma\, n_o T_{RIC}}\right)\left(\frac{m_e^*}{3k_B T}\right)^{1/2}\right]^{\Delta(T)} \left[2\left(\frac{\sqrt{m_e^* m_h^*}\, k_B T}{2\pi\hbar^2}\right)^{3/2}\right]^{1-\Delta(T)} = k_{RICo} \cdot k_{RIC1}{}^{\Delta(T/T_{RIC})} \left[T/T_{RIC}\right]^{3/2-2\cdot\Delta(T/T_{RIC})} \tag{9}$$

$$with \quad k_{RICo} \equiv \left[\frac{q_e \mu_o}{\pi\sqrt{2\pi}\,\hbar^3}\left(m_e^* m_h^*\right)^{3/4}\left(k_B T_{RIC}\right)^{3/2}\right] \quad and \quad k_{RIC1} \equiv \left[\left(\frac{\pi\sqrt{2\pi}\,\rho_m\, k_B\, \hbar^3}{\sqrt{3}\, s\Sigma\, n_o}\right)\left(\frac{\sqrt{m_e^*}}{\left(m_e^* m_h^*\right)^{3/4}}\right)\left(k_B T_{RIC}\right)^{-3}\right]$$

Here, $s$ is the capture cross section of conduction electrons by fixed holes, $\Sigma$ is the average energy absorbed to excite an electron from the valence band into the conduction band; $m_e$*, and $m_h$* are the electron and hole effective masses; and $\rho_m$ is the mass density.

$k_{RIC}$ can be expressed in more compact notation as a power law expression of the reduced temperature, $T/T_{RIC}$, with two parameters $k_{RICo}$ and $k_{RIC1}$. The temperature-independent RIC magnitude, $k_{RICo}$, is proportional to the electron mobility, $\mu_o$ which is typically assumed to be independent of $T$.[17,23,28,31,41] The temperature-dependent RIC magnitude, $k_{RIC1}$, is proportional to the probability of carrier electrons in the conduction band and scales as the inverse of the product $(s\ \Sigma\ n_o)$. It follows trivially from the reduced form of Eq. (8) that at $T \ll T_{RIC}$ where $\Delta \rightarrow 1$ then $k_{RIC}$ is proportional to $[T/T_{RIC}]^{-1/2}$ and that when $T \rightarrow T_{RIC}$ where $\Delta \rightarrow ½$ then $k_{RIC}$ is proportional to $[T/T_{RIC}]^{1/2}$. Harrison noted that amorphous materials tend to have $\Delta \rightarrow 1$, while highly crystalline materials tend to have $\Delta \rightarrow ½$.[43]

Figure 5 shows parametric sets of curves of the temperature dependence of the RIC parameters $k_{RIC}$ and $\Delta$ evaluated for $T_{RIC}$ from 200 K to 1000 K. Note that the flat regions in the curves of Figure 5 occur when $T > T_{RIC}$ and $\Delta$ is fixed to a value of ½.

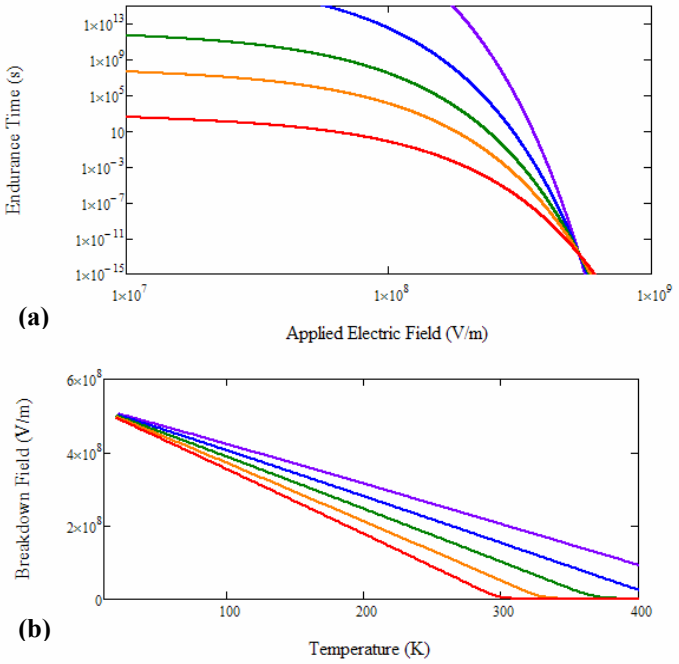


**Figure 6. Temperature dependence of the electrostatic field breakdown strength.** ***(a)*** *Endurance, or time to breakdown, a function of applied electric field, based on Eq. (9). Curves shown are for temperature set to 150 K (purple), 200 K (blue), 250 K (green), 300 K (orange) and 400 K (red).* ***(b)*** *Breakdown field strength as a function of temperature, based on Eq. (10). Curves shown are endurance times set to $10^0$ s (purple), $10^2$ s (blue), $10^4$ s or 2.8 hr (green), $10^6$ s or 11.6 days (orange) and $10^8$ s or 3.2 yr (red). To approximately match LDPE data, we have set $F_{ESD}=9.5\cdot10^8$ V/m and $\Delta G=1.22$ eV.*

### D. Electrostatic Discharge Field Strength

A thermodynamic model for the electric field aging process has been proposed by Cline *et al.* to predict the mean time to failure or endurance time, $t_{en}$, as a function of high electric field and temperature.[44,45] The model has two parameters: the maximum size of submicrocavities, $\lambda$, and the change in Gibbs free energy, $\Delta G$, for a

rupture of interchain van der Waals bonds or the activation energy of the chain deformation or micro-void formation process.[18] There are direct equivalences between the thermodynamic model[44,45] for electrostatic breakdown and Mott's model for TAH conductivity.[27] As with the TAH model, $\lambda$ and $\Delta G$ represent a mean separation of sites (or barrier width) and an activation energy (or barrier height of the energy well), respectively. [E3]

The transition probability to break an interchain bond is equal to the reciprocal of the endurance time, $P=1/t_{en}$. The average drift velocity, equal to the mean distance traveled divided by endurance time, $\lambda/t_{en}$, and is by definition also equal to $\mu F$; solving for $P$ then, $1/t_{en}=(\mu/\lambda)E$. $P$ also corresponds to the mean hop frequency, $\nu_{TAH}$; thus, $h/t_{en}$ can be thought of as the quantum energy uncertainty for a broken bond. An expression similar to the TAH mobility term in Eq. (2) follows by setting the transition probability to unity as $F \rightarrow F_{ESD}$, that is

$$1 = \left(\frac{k_B T}{h/t_{en}}\right)\exp\left[\frac{-\Delta G}{k_B T}\right]\sinh\left[\frac{q_e F_{ESD}\,\lambda}{k_B T}\right] = \left(\frac{k_B T}{h/t_{en}}\right)\left(\frac{\frac{3}{4}F_{ESD}}{F_{A'}}\right)\left[\frac{T_{A'}}{T}Z_{A'}(\beta_{A'})\exp\left[\frac{-T_{A'}}{T}\right]\right]$$
$$\text{with} \quad \beta_{A'} \equiv \tfrac{4}{3}F_{ESD}\,T_{A'}/F_{A'}\,T \rightarrow q_e F_{ESD}\,\lambda/k_B T \quad \text{and} \quad Z_A(\beta_A) \equiv \frac{1}{\beta_A}\sinh(\beta_A) \tag{10}$$
$$\text{plus} \quad T_{A'} \equiv \Delta G/k_B \qquad \text{and} \qquad F_{A'} \equiv \Delta G/q_e\left(\tfrac{3}{4}\lambda\right) \rightarrow \tfrac{3}{4}F_{ESD}$$

Here the carrier mobility is proportional to a Boltzmann factor with the energy scale set by trap depth, $\Delta G$. The carrier mobility is also proportional to the difference in the rates of breaking bonds and bond rebounding [or equivalently, a Boltzmann factor with energy scale $\pm q_e F\lambda$ gained (lost) by a charge carrier moving with (against) the electric field over a distance of the average trap separation, $\lambda$]. This results in the hyperbolic function in Eq. (10),[44] in a manner reminiscent of the early hopping conductivity work of Miller and Abrhams.[35] Solving for $F_{ESD}$ in terms of $t_{en}$, the temperature, and the model parameters $\lambda$ and $\Delta G$ (or equivalently the reduced parameters $T_{A'}$ and $F_{A'}$),

$$F_{ESD} = \left[\frac{k_B T}{q_e\left(\frac{3}{4}\lambda\right)}\right]\csc h^{-1}\left[\left(\frac{h/t_{en}}{k_B T}\right)\exp\left(\frac{\Delta G}{k_B T}\right)\right] = \left(\tfrac{3}{4}F_{A'}\frac{T}{T_{A'}}\right)\csc h^{-1}\left[\left(\frac{h/t_{en}}{k_B T}\right)\exp\left(\frac{-T_{A'}}{T}\right)\right] \tag{11}$$

At breakdown, the energy gained from electron motion through the electric field across a micro-void of width λ, $q_e F_{ESD}\lambda$ is just sufficient to overcome the barrier height $\Delta G$; from Eq. (10) then, $F_{ESD} = \frac{4}{3}F_{A'}$ or equivalently $a=\frac{3}{4}\lambda$.

Griffiths[18] and Dang[45] review alternate theories relating the endurance to the electrostatic break down and temperature, such as the more simple inverse power law model and the more complete electrokinetic endurance model[E13] that predicts a threshold value for electrostatic breakdown at long endurance times. All these theories predict roughly similar values for endurance and approximately similar temperature dependence in the range of endurance times typically measured by experimental tests, that is in the range of $10^0$ to $10^6$ s.[18]

## IV. Application to Low-Density Polyethylene

Figure 6 shows plots of the total conductivity and component conductivities as functions of $F$, $T$ and $\dot{D}$ from the engineering tool for low-density polyethylene (LDPE), as a representative material. Figures 6(a-c) show the total conductivity, $\sigma_{Total}$, as a function of $F$ and $T$ at: (a) low, $\dot{D} \rightarrow 0$; (b) intermediate, $\dot{D} = 5\cdot10^{-3}$ Rad/s; and (c) high, $\dot{D} =$ 0.27 Rad/s dose rates. Figures 6(d-f) show the individual components $\sigma_{TAH}$ and $\sigma_{VRH}$ as functions of $F$ and $T$ and $\sigma_{RIC}$ as a function of $\dot{D}$ and $T$. $\sigma_{RIC}$ is seen to dominate $\sigma_{Total}$ at low $T$, $\sigma_{TAH}$ dominates at higher $T$ and lower $F$, and $\sigma_{VRH}$ dominates at higher $T$ and higher $F$.

LDPE is one of the most common and versatile polymers; high uniformity and high purity samples can easily be obtained for testing. Much is known about the structure and properties of LDPE[16,46-49] and it is relatively well characterized. LDPE is semi-crystalline, which increases the likelihood that hopping conductivity is an appropriate model. The relatively high steady-state conductivity of LDPE at room temperature, on the order of $10^{-15} - 10^{-18}$ $(\Omega\text{-cm})^{-1}$,[50] means it is measurable using constant voltage conductivity test methods even at low temperatures.

An extensive data set has been taken by the Utah State University Materials Physics Group [ref 5-7] which has been compared to other data available in the literature.[16,46-49] Samples of branched LDPE (Goodfellow, ASTM type I)[50] of (27.4±0.2) μm thickness had a density of 0.92 g/cm$^3$ with an estimated crystallinity of 50% ,[17] and a relative dielectric constant of 2.26.[17] All samples were chemically cleaned with methanol prior to a bakeout at 65(±1) $^o$C under ~$10^{-3}$ Pa vacuum for >24 hr to eliminate absorbed water and volatile contaminants; samples conditioned in this manner had a measured outgassing rate of < 0.05% mass loss/day at the end of bakeout as determined with a modified ASTM 495 test procedure.[51] USU dark current conductivity experiments were conducted at room

temperature for electric fields ranging was from $8 \cdot 10^4$ V-m$^{-1}$ to $2.7 \cdot 10^8$ V-m$^{-1}$ (or from <0.05% up to ~92% of $F_{ESD}$) and over a temperature range of ~120 K to 345 K at ~$4 \cdot 10^6$ V-m$^{-1}$. No charge storage conductivity measurements have been made to date.

RIC was measured for adsorbed dose rate over a range of $10^{-5}$ Gray to $10^{-1}$ Gray at 5 fixed temperatures from 126 K to 357 K.[14,52] The measured data clearly showed the power law behavior of Eq. (7) as each fixed temperature. Measured values of $\Delta$ are in the range of $0.5 < \Delta < 1.0$, as expected. Above ~250 K, the temperature dependence of $k_{RIC}$ and $\Delta$ were reasonably consistent with Eqs. (8) and (9) developed for photoconductivity models of localized trap states in disordered semiconductors. The temperature behavior of $\Delta$ above ~250 K is modeled reasonably well by Eq. (8) with $T_{RIC}$=600 K and is consistent—to within experimental uncertainties—with numerous previous studies above ~253 K.[28,53-56] The average measured value of $k_{RIC}$ at room temperature value of $(2 \pm 1) \cdot 10^{-12}$ (Gr sec$^{-1}$ Ω m)$^{-1}$ is in reasonable agreement with the range of $(3 \text{ to } 6) \cdot 10^{-12}$ (Gr sec$^{-1}$ Ω m)$^{-1}$ from previous studies.[28,55,56] The temperature behavior of $k_{RIC}$ shown in Fig. 3b is in good agreement with previous temperature studies extending over a range of ~120 K to 355 K,[28,53,57] when these studies are normalized to the same $k_{RIC}$ at room temperature to account for modest differences in materials and methods.[16]

Below ~250 K, $k_{RIC}$ and $\Delta$ exhibited little change with temperature. Below ~250 K, $\Delta$ had a constant value of 1.0. Fowler reported below ~250 K a similar jump in $\Delta$ to a constant value of 0.83. The observed abrupt changes in temperature dependence for RIC at ~253 K (ref. R4) and in dark current conductivity at 268±2 K (ref. B18) may well be related to a LDPE structural phase transition seen at 250 K<$T_\beta$<262 K in prior studies of mechanical and thermodynamic properties. The β transition is a structural phase transition routinely observed in branched PE, which has been associated with conformational changes along polymer chains in the interfacial matrix of disordered polymer between nanocrystalline regions in the bulk.[B26]

Electrostatic breakdown field strength of conditioned samples was measured in a separate test chamber to be 2.9(±0.3) $10^8$ V/m, using a modified ASTM D 3755 test procedure at room temperature under <$10^{-2}$ Pa vacuum with a voltage ramp rate of 20 V steps each sec. Griffiths[18] reported a more complete study of the electrostatic breakdown of cross linked polyethylene and fits to the data based on inverse power law, thermodynamic,[44,45] and electrokinetic endurance models.[59] They found a value for the bond deformation activation energy, $\Delta G$, of 1.2 eV. Based on their room temperature data and our Eq. (11), we estimate the maximum size of involved in electrostatic breakdown, $\lambda$, to be 0.6 nm=0.735 $a$, or equivalently, in excellent agreement with the prediction from Section III. D.

Based on the best overall fits to the full data set, using Eqs. (2) through (9), we estimate the fitting parameters to be:

| | | |
|---|---|---|
| $\sigma_{TAHo} = 1.4 \cdot 10^{-10}$ (Ω-cm)$^{-1}$ | $\sigma_{VRHo} = 1.0 \cdot 10^{-10}$ (Ω-cm)$^{-1}$ | $k_{RICo} = 1.8 \cdot 10^{-14}$ (Ω-cm-Rad/sec)$^{-1}$ |
| $E_A = 9.5 \cdot 10^8$ V/m | $E_V = 6.9 \cdot 10^{13}$ V/m | $k_{RIC1} = 4.6 \cdot 10^{-5}$ |
| $T_A = 6626$ K | $T_V = 1.0 \cdot 10^8$ K | $T_{RIC} = 600$ K.. |
| $\Delta G$=1.2 eV | | |

Based on Eq. (3b), Eq. (4) and Eq. (10) these fitting parameters correspond to:

| | |
|---|---|
| Average well spacing $a$=0.8 nm | Average well depth $\Delta H$=0.57 eV |
| Localization decay length $\alpha^{-1}$=2.9 nm | Average RIC energy $\Delta W$=8.8 keV |
| | Effective Fermi separation, $E_b$=0.052 eV |
| Submicrocavities cavity size $\lambda$, to be 0.6 nm | Bond breaking energy $\Delta G$, of 1.2 eV |

These values are in surprisingly good agreement with activation energy or an average well separation $\Delta H$ of 0.78 eV [48]; 0.87 eV [46]; 0.80 eV to 0.83 eV [48]; and 0.6 eV to 1.1 eV [47] from previous studies of LDPE conduction. and a trap site separation (2.8 nm [46] and 2.0 eV at 303 K [47]) from previous studies of LDPE conduction.

## Acknowledgments

The invaluable contributions to instrumentation design and data analysis made by Anthony Thomas, Ryan Hoffmann, Joshua Hodges, Jonathon Abbott and Prasanna Swaminathan and to sample preparation and characterization by Amberly Evans and Johnathon Tippetts are gratefully acknowledged. This work was supported by a project for the James Web Space Telescope Electrical Systems Group through the NASA Goddard Space Flight Center.

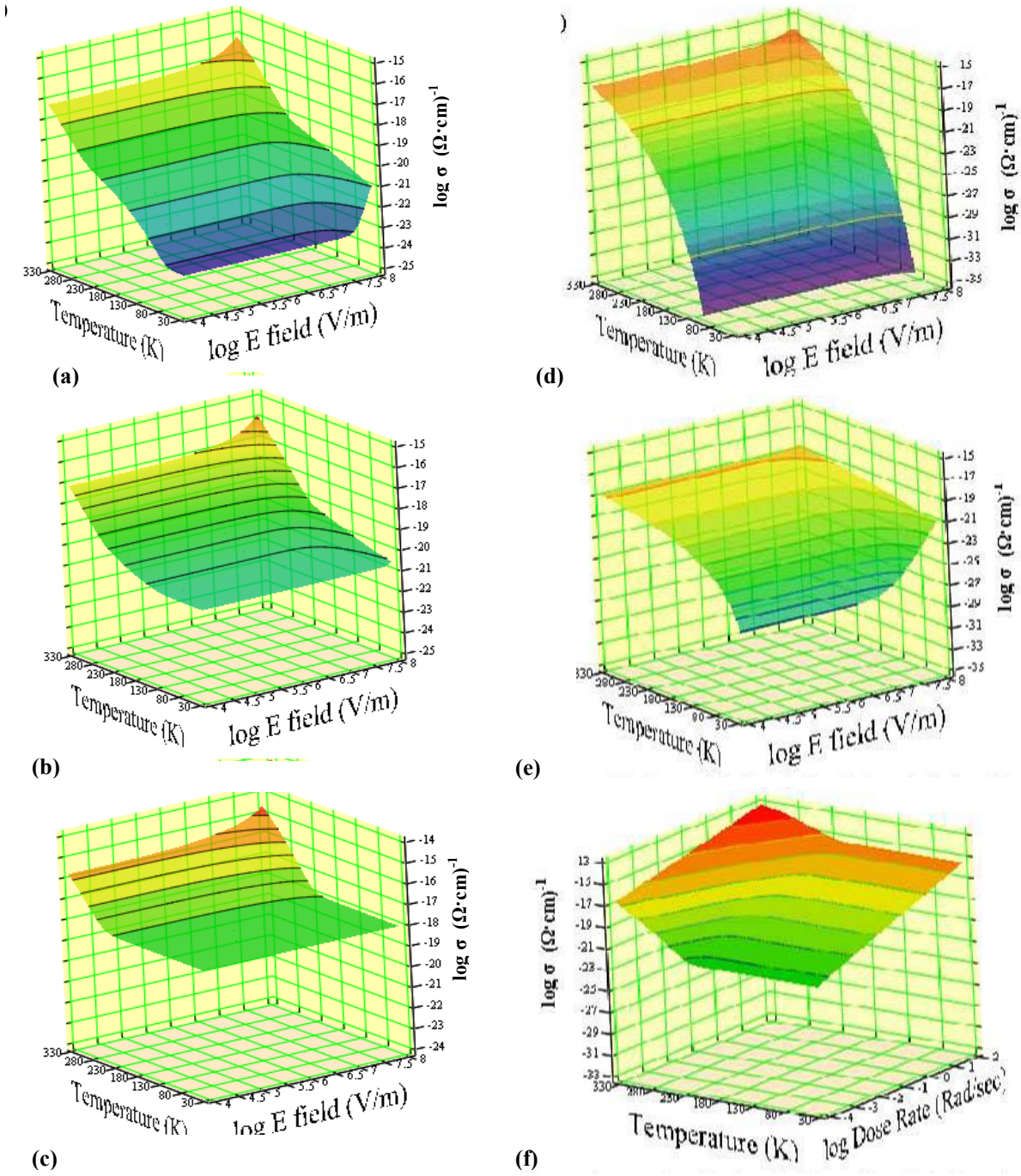


**Figure 6. Total conductivity and component conductivities as functions of *F*, *T* and $\dot{D}$ from the engineering tool for low-density polyethylene (LDPE).** ***(a-c)*** *Total conductivity of LDPE as a function of F and T at:* ***(a)*** *low,* $\dot{D} \rightarrow 0$; ***(b)*** *intermediate,* $\dot{D} = 5 \cdot 10^{-3}$ *Rad/s; and* ***(c)*** *high,* $\dot{D} = 0.27$ *Rad/s dose rates.* ***(d-f)*** *Individual components:* ***(d)*** $\sigma_{TAH}$ *as functions of F and T;* ***(e)*** $\sigma_{VRH}$ *as functions of F and T ; and* ***(f)*** $\sigma_{RIC}$ *as a function of* $\dot{D}$ *and T.* $\sigma_{RIC}$ *is seen to dominate* $\sigma_{Total}$ *at low T,* $\sigma_{TAH}$ *dominates at higher T and lower F, and* $\sigma_{VRH}$ *dominates at higher T and higher F. To approximately match LDPE data, we have set* $\sigma_{TAHo}=1.4 \cdot 10^{-10}$ $(\Omega\text{-cm})^{-1}$, $F_A=9.5 \cdot 10^{8}$ *V/m and* $T_A=6626$ *K;* $\sigma_{VRHo}=1.0 \cdot 10^{-10}$ $(\Omega\text{-cm})^{-1}$, $F_V=6.9 \cdot 10^{13}$ *V/m and* $T_V=1.0 \cdot 10^{8}$ *K; and* $k_{RICo}=1.8 \cdot 10^{-14}$ $(\Omega\text{-cm-Rad/sec})^{-1}$ *and* $k_{RIC1}=4.6 \cdot 10^{-5}$ *for* $T_{RIC}=600$ *K.*

## References


[1]D. Hastings, H. Garrett, *Spacecraft-Environment Interactions,* New York, NY: Cambridge Press, 1996.

[2]J.R. Dennison, C.D. Thomson, J. Kite, V. Zavyalov, and Jodie Corbridge, "Materials Characterization at Utah State University: Facilities and Knowledgebase of Electronic Properties of Materials Applicable to Spacecraft Charging," *Proceedings of the 8th Spacecraft Charging Technology Conference,* (NASA Marshall Space Flight Center, Huntsville, AL, October 2003).

[3]R.D Leach and M.B. Alexander, "Failures and anomalies attributed to spacecraft charging," NASA Reference Publication 1375, NASA Marshall Space Flight Center, August 1995.

[4]A.R. Frederickson and C.E. Benson, "Improved Testing Procedures For Spacecraft Discharge", *Proceedings of the 7th Spacecraft Charging Technology Conference,* (ESTEC, Noordwijk, The Netherlands, April 2001).

[5]J.R. Dennison, A.R. Frederickson, and Prasanna Swaminathan, "Charge Storage, Conductivity, and Charge Profiles of Insulators As Related to Spacecraft Charging," *Proceedings of the 8th Spacecraft Charging Technology Conference,* (NASA Marshall Space Flight Center, Huntsville, AL, October 2003).

[6]A.R. Frederickson and J.R. Dennison, "Measurement of Conductivity and Charge Storage in Insulators Related to Spacecraft Charging," *IEEE Transaction on Nuclear Science,* 50(6), 2284-2291 (December 2003).

[7]J.R. Dennison and J. Brunson, *IEEE Trans. Plasma Sci.* **36** (2008).

[8]J.R. Dennison, Prasanna Swaminathan, Randy Jost, and Jerilyn Brunson, Nelson W. Green, and A. Robb Frederickson, "Proposed Modifications To Engineering Design Guidelines Related To Resistivity Measurements And Spacecraft Charging," *Proceedings of the 9th Spacecraft Charging Technology Conference,* (Epochal Tsukuba, Tsukuba, Japab, April 4-8, 2005).

[9]J.R. Dennison, Prasanna Swaminathan, Randy Jost, Jerilyn Brunson, Nelson Green, and A. Robb Frederickson, "Improved Methods and Analysis for Resistivity Measurements Related to Spacecraft Charging," *IEEE Transaction on Plasma Science,* 34(5) October 2006, 2191-2203.

[10]Nelson W. Green and JR Dennison, "Deep Dielectric Charging of Spacecraft Polymers by Energetic Protons," *IEEE Transaction on Plasma Science,* **36**(5) October 2008, 2482-2490.

[11]Dan Arnfield, Senior Project, "The Effect of Temperature on Dielectric Breakdown of Kapton HN," Utah State Un., Logan, UT, 2008.

[12]Anthony Thomas, Senior Project, "The Effect of Voltage Ramp Rate on Dielectric Breakdown of Thin Film Polymers," Utah State Un., Logan, UT, 2007..

[13]ASTM D 3755, "Standard Test Method for Dielectric Breakdown Voltage and Dielectric Strength of Solid Electrical Insulating Materials under Direct-Voltage Stress," West Conshohocken, PA: American Society for Testing and Materials, 2001.

[14]JR Dennison, Jodie Gillespie, Joshua Hodges, RC Hoffmann, J Abbott, Alan W. Hunt and Randy Spalding, "Radiation Induced Conductivity of Highly-Insulating Spacecraft Materials," *Proceedings of the 10th Spacecraft Charging and Technology Conference, (*Biarritz, France, June 18-21, 2007).

[15]F.J. Campbell "Radiation Effects of the Electrical Properties of Solid Insulation," *in Engineering Dielectrics – Volume IIA: Electrical Properties of Solid Insulating Materials: Molecular Structure and Electrical Behavior, American Society for*

[16]V. Adamec and J. H. Calderwood, "On the determination of electrical conductivity in polyethylene," J. Phys. D: Appl. Phys., 14, 1487-1494, 1981.

[17]H.J. Wintle, "Conduction Processes in Polymers," *in Engineering Dielectrics – Volume IIA: Electrical Properties of Solid Insulating Materials: Molecular Structure and Electrical Behavior, American Society for Testing and Materials,* R. Bartnikas, Editors, (American Society for Testing and Materials, Philadelphia, PA 19103, 1983).

[18]C.L. Griffiths, J. Freestone, R.N. Hampton, "Thermoelectric Aging of Cable Grade XLPE," Conf. Record of IEEE International Symposium on Electrical Insulation, Arlington, VA, 1998, pp. 578-582.

[19]R. Zallen,, *The Physics of Amorphous Solids*, New York: Wiley, 1983, p. 252.

[20] V.I. Arkhipov, Phys. Rev. Lett., 82, 1321, 1999.

[21]V.I. Arkhipov, Charge Transport in Organic Semiconductors, in Phtophysics of Molecular Materials, pp.261-366,2006.

[22]A.P. Tyutnev, "Radiation-induced Conductivity of Polymers: A Review," High Energy Chem. 30(1), pp. 1-13, 1996.

[23]A.P. Tyutnev, V.S. Saenko, E.D. Pozhidaev and V. A. Kolesnikov, *High Performance Polymers*, 17 (2005) 175-192..

[24]H. Bassler, Physical Status of Solid B, 175, 15-56, 1993.

*Testing and Materials,* R. Bartnikas, Editors, Philadelphia: Am. Soc. for Testing and Materials, 1983.

[25]N.F. Mott, Phil. Mag. 19, 835 (1969).

[26]H.N. Poole, *Philosophical Magazine,* 34, 195-204, 1917.

[27]N.F. Mott and E.A. Davis, *Electronic Processes in Non-Crystalline Materials,* 2nd Ed. (Oxford University Press, Oxford, 1979).

[28]J. F. Fowler, *Proc. Royal Soc. London A,* **23**, 464 (1956).

[29]J.F. Fowler, "X-ray Induced Conductivity in Insulating Materials," Ph.D. Thesis, Un. London, 1955.

[30]P.W. Anderson, Phys. Rev., 109, 1492, 1958.

[32] H. Scher and E.W. Montroll, Phys. Rev. B, 12, 2455, 1975.

[33]D.H. Dunlap, P.E. Harris, V.M Kenkre, Phys. Rev. Lett., 77,542, 1996.

[34]A. Miller and E. Abrhams, Phys. Rev. 120,745, 1960.

[35]A. T. Amos and R. J. Crispin, J. Chem. Phys., 63, 1890-1899, 1975.

[36]H. Böttger and V.V. Bryskin, *Hopping Conduction in Solids.* (Akademie-Verlag, Berlin, 1985).

[37]N Apsley and P H Hughes, "Temperature- and field-dependence of hopping conduction in disordered systems," *Phil. Mag.* **30** 963-972, 1974.

[38]N. Apsley and P H Hughes, "Temperature- and field-dependence of hopping conduction in disordered systems, II," *Phil. Mag.* **31** 1327-1339, 1975.

[39]L. Weaver, J. Kenneth Shultis, and R. E. Faw, *J. Appl. Phys.* **48,** 2762 (1977).

[40]A. Chapiro, *Atomic Radiation and Polymers*, New York: Pergamon, (1960) p. 171.

[41]A. Rose, *RCA Rev.*, **12**, 362 (1951).

[42]S.E Vaiserburg, *Radiation Chemistry of Physics*, Kragin, V.A.M Ed., Moscow:Naaka,1973.

[43]S.E. Harrison, "A Study of Gamma-Ray Photoconductivity in Organic Dielectric Materials," MS Thesis, Un. New Mexico, 1962.

[44] J.-L. Parpal, J.P. Crine, C. Dang, "Electrical Aging of Extruded Dielectric Cables: A Physical Model," IEEE Trans. Dielectrics and Insulators, Vol. 3, No. 2, April 1996, 197-209.

[45]C. Dang, J.-L. Parpal, J.P. Crine, "Electrical Aging of Extruded Dielectric Cables: Review of Existing Theory and Data," IEEE Trans. Dielectrics and Insulators, Vol. 3, No. 2, April 1996, 237-247.

[46]Nath and M. M. Perlman, "Steady-state bulk trap-modulated hopping conduction in doped linear low-density polyethylene," J. Appl. Phys. 65, 4854-4858, 1989.

[47]L. Boudou and J. Guastavino, "Influence of temperature on low-density polyethylene films through conduction measurement," J. Phys. D: Appl Phys. 35, 1555-1561, 2002.

[48]J. N Marat-Mendes, R. M. Neagu and E. R. Neagu, "Electrical conduction and space charge trapping in highly insulating materials," J. Phys. D: Appl. Phys, 37, 343-347, 2004.

[49]G.C. Montanari, G. Mazzanti, F. Palmieri, A. Motori, G. Perego and S. Serra, « Space-charge trapping and conduction in LDPE, HDPE and XLPE," J. Phys. D: Appl. Phys., 34, 2902-2911, 2001.

[50]"Material Information – Polyethylene Low Density LDPE," .Goodfellow, Devon, PA, January 20, 2006.

[51]ASTM D 495-99, "Standard Test Method for High-Voltage, Low-Current, Dry Arc Resistance of Solid Electrical Insulation," West Conshohocken, PA: American Society for Testing and Materials, 2001.

[52]JR Dennison, Jodie Gillespie, Joshua Hodges, RC Hoffmann, J Abbott, Alan W. Hunt and Randy Spalding, "Radiation Induced Conductivity of Highly-Insulating Spacecraft Materials," submitted to *Nuclear Instruments and Methods in Physics Research B*.

[53]K. Yahagi and A. Danno, *J. Appl. Phys.*, **34,** 804 (1963).

[54]S. Mayburg and W.L. Lawrence, *J. Appl. Phys*. **23**, 1006 (1956).

[55]J.H. Coleman and D. Bohm, *J. Appl. Phys.* **24,** 497 (1953).

[56]C.L. Hanks and D.J. Hammond, *REIC Report No. 46*, Columbus, OH: Radiation Effects Center, 1969. p. 39.

[57]R.A. Myer, F.L. Bouquet, R.S. Alger, J. App. Sci. Phys.,27(9),1012, (1956).[58]R. Popli, M. Glotin, L. Mandelkern, and R.S. Benson, *J. Polymer Sci. Polymer Phys. Ed,* **22,** 407 (1984).

[59]T.J. Lewis., Llewellyn, J.P. van der Sluijs, M.J., Freestone, J. and Hampton, R.N., 1996, Seventh International Conference on Dielectric Materials Measurement and Applications, 23-26 September, IEE Conference Publication Number 430, pp220-224.